Regionally Specific Brain Volumetric and Cortical Thickness Changes in HIV-infected Patients in the HAART era

Ryan Sanford, MSc[a,*], **Ana Lucia Fernandez Cruz, MSc**[a], **Susan C. Scott, PhD**[c], **Nancy E. Mayo, PhD**[c], **Lesley K. Fellows, MD CM, DPhil**[a], **Beau M. Ances, MD, PhD**[b,+], and **D. Louis Collins, PhD**[b,+]

[a]Montreal Neurological Institute, McGill University, 3801 University Street, Montréal, Québec, Canada H3A 2B4

[b]Department of Neurology, Washington University, Box 8111, 660 South Euclid, St. Louis, Missouri, USA 63110

[c]Division of Clinical Epidemiology, McGill University, Montreal, Quebec, Canada

Abstract

Background—Cognitive impairment still occurs in a substantial subset of HIV-infected patients, despite effective viral suppression with highly active antiretroviral therapy (HAART). Structural brain changes may provide clues about the underlying pathophysiology. This study provides a detailed spatial characterization of the pattern and extent of brain volume changes associated with HIV, and relates these brain measures to cognitive ability and clinical variables.

Methods—Multiple novel neuroimaging techniques (deformation-based morphometry, voxel-based morphometry and cortical modeling) were used to assess regional brain volumes in 125 HIV-infected patients and 62 HIV-uninfected individuals. 90% of the HIV-infected patients were on stable HAART with a majority (75%) having plasma viral suppression. Brain volumetrics and cortical thickness estimates were compared between the HIV-infected and uninfected groups, and the relationships between these measures of brain volume and indices of current and past infection severity, central nervous system penetration of HAART, and cognitive performance were assessed.

Results—Regionally specific patterns of reduced thalamic and brainstem volumes, as well as reduced cortical thickness in the orbitofrontal cortex, cingulate gyrus, primary motor and sensory cortex, temporal, and frontal lobes were seen in HIV-infected patients compared to HIV-uninfected participants. Observed white matter loss and subcortical atrophy were associated with lower nadir CD4 cell counts, while reduction in cortical thickness was related to worse cognitive performance.

Conclusion—Our findings suggest that distinct mechanisms may underlie cortical and subcortical injury in people with HIV, and argues for the potential importance of early initiation of HAART to protect long term brain health.

Keywords

Magnetic Resonance Imaging; Deformation-based morphometry; Voxel-based morphometry; Cortical modeling; HIV-associated neurocognitive disorders

Introduction

The introduction of highly active antiretroviral therapy (HAART) has successfully shifted HIV from a terminal illness to a manageable chronic condition. However, the prevalence of mild-to-moderate cognitive impairment due to HIV has not declined, with up to 40% of HIV-infected patients affected despite effective viral suppression and minimal comorbidities [1]. The underlying pathogenesis of brain dysfunction remains unclear with several proposed mechanisms, including: permanent damage prior to HAART initiation, ongoing brain injury from low level viral replication and immune activation despite effective viral control, presence of comorbid neurological or psychiatric conditions, and HAART neurotoxicity [2].

Neuroimaging studies in the HAART era have reported brain volume loss in various cortical and subcortical regions [3,4]. Despite a growing body of studies, the patterns and spatial distribution of brain injury remains unclear [5]. For example, increased putamen volume was detected in HIV-infected individuals compared to an age- and education-matched HIV-uninfected group [6], while other studies have reported decreased putamen volume [7,8]. Likewise, there is no clear consensus on the existence or extent of cortical effects in HIV, with some studies reporting significant cortical atrophy [9-11], while others have detected no cortical differences [12,13]. These inconsistencies could reflect heterogeneity of both HIV-infected (i.e. degree of infection and impairment severity) and HIV-uninfected (i.e. poorly matched controls) groups across studies, variations in the methods used to estimate brain volumes, and/or differences in the brain regions investigated. Much of this work has involved small samples, often necessitating region-of-interest designs that constrain their anatomical scope.

The present study aimed to provide a detailed spatial characterization of the pattern and extent of brain volume changes in a cohort of HIV-infected patients and a demographically-matched HIV-uninfected group. Multiple novel neuroimaging methods with complementary strengths (deformation-based morphometry (DBM), voxel-based morphometry (VBM) and cortical modeling) were applied to this large sample to assess the relationship between regionally specific brain volume estimates and HIV status, measures of current and past infection severity, treatment effects, and cognitive function.

Methods

Subjects

HIV-infected participants were recruited from the infectious disease clinic at Washington University in St. Louis (WUSTL), while HIV-uninfected participants with similar sociodemographic factors were recruited from the local community by leaflets. All participants provided written consent approved by the WUSTL Institutional Review Board.

Participants were excluded from the study if they had a history of confounding neurological disorders including epilepsy, dementia or stroke, current or past opportunistic central nervous system infection, traumatic brain injury (loss of consciousness >30 minutes), major psychiatric disorders including schizophrenia, depression, bipolar disorder or obsessive-compulsive disorder, or active substance abuse and dependence diagnosis according to Diagnostic and Statistics Manual of Mental Disorders 4th edition criteria. Individuals with past substance use were not excluded. All participants who met these criteria, had laboratory evaluations (current plasma CD4 cell count and viral load), and completed magnetic resonance imaging (MRI) and neuropsychological tests were included in the analysis. This yielded a total of 133 HIV-infected and 66 HIV-uninfected participants. For all HIV-infected patients receiving HAART, a central nervous system penetration effectiveness (CPE) score was generated based on previous methods [14].

Neuropsychological evaluation

Ninety-eight HIV-infected and 47 HIV-uninfected participants completed an extensive neuropsychological assessment: Timed Gait, Grooved Pegboard (dominant and non-dominant), Hopkins Verbal Learning Test Revised, Trail-Making Tests A/B, Digit-Symbol, Stroop Colour and Words, Stroop Interference, Letter Number Sequencing, and Verbal Fluency. An additional 35 HIV-infected and 19 HIV-uninfected participants completed a briefer neuropsychological assessment (due to logistical reasons): Trail-Making Tests A/B, Hopkins Verbal Learning Test Revised, and Digit-Symbol. Two approaches were taken to summarize overall test performance. The conventional method generates Z-scores from each test using demographic (age, gender, ethnicity, and education) adjusted normative means [15]. Z-scores from four tests available in the whole sample (Trail-Making Tests A/B, Hopkins Verbal Learning Test Revised, and Digit-Symbol) were averaged to generate a summary Z-score (NPZ-4). However, the NPZ-4 has limitations: the available norms may not be appropriate for all individuals studied, and averaging can reduce informative variance, posing potential difficulties in its use for statistical analysis [16]. An alternative approach, Rasch analysis, uses item-response theory to determine the extent to which a set of items (i.e. neuropsychological tests) and responses to those items reflect a single latent construct (i.e. cognitive ability) [16]. Rasch analysis arranges items and participant responses on the same scale (logits)such that items that most participants pass are considered easy items and participants who fail to pass them are considered to have less cognitive ability. Similarly, items that few participants pass are harder items and participants who pass them have more cognitive ability [16]. The result is an estimate of each person's cognitive ability that can be treated as a continuous ruler-like measure, and does not require demographic norms. This approach also accommodates missing data, allowing it to be applied on all available neuropsychological test scores for this sample (supplementary material). Since the Rasch approach generates a continuous ruler-like measure of cognitive ability, it is more suitable for parametric statistical testing and was therefore used to test brain structure-function relationships [16].

Magnetic resonance imaging acquisition and analyses

All participants underwent contemporaneous MRI using the same 3T Siemens Tim TRIO whole-body magnetic resonance scanner (Siemens AG, Erlangen, Germany) with a 12

channel transmit/receive head coil. The scanning protocol included T_1-weighted three-dimensional magnetization-prepared rapid acquisition gradient echo (MPRAGE) sequence [repetition time (TR)/echo time (TE)/inversion time (TI) = 2400/3.16/1000 ms, flip angle = 8°, and voxel size = 1 mm^3], and a T_2-weighted SPC sequence [TR/TE=3200/460 ms, flip angle = 120°, and voxel size = 1 mm^3]. The same scanning protocol was used for all participants. All acquired MRI were visually inspected at the scanner with an additional scan performed if significant movement or artifact was observed.

Pre-processing of all scans included denoising with optimized non-local means filtering [17], correction for intensity inhomogeneity [18], brain masking [19], and linear intensity scaling using histogram matching to the Montreal Neurological Institute (MNI) 152 average brain template. The resulting images were linearly registered to the MNI152 template using a nine-parameter affine transform to correct for variations in head size, position, and orientation [20]. Following these pre-processing steps, all MRI data was carefully inspected for significant structural brain abnormalities, white matter hyperintensities from the T_2-weighted images, and unacceptable image processing outcomes. This resulted in the removal of 8 HIV-infected and 4 HIV-uninfected participants from subsequent analysis, yielding a final total of 125 HIV-infected and 62 HIV-uninfected participants. Following visual quality control, the T_1-weighted data for all participants was available for VBM, DBM and cortical modeling as described below.

The use of VBM, DBM and cortical modeling is advantageous because they provide complementary information about brain volumes, that is, VBM and DBM are better suited to detect subcortical changes associated with tissue densities and anatomical size (i.e. volume), respectively, while cortical modeling can capture subtle cortical thickness changes. Combining these methods maximizes brain volume information, so regionally specific brain changes can be optimally detected in cortical and subcortical regions.

Voxel-based morphometry

VBM identifies local tissue density changes in gray matter (GM), white matter (WM), and cerebrospinal fluid (CSF) space [21]. The pre-processed T_1-weighted data was spatially normalized to the MNI152 space. An artificial neural network classifier categorized each voxel into one of three classes: GM, WM, and CSF [22]. Each tissue map was smoothed with an isotropic Gaussian kernel of 8 mm full width half maximum (FWHM). The resulting maps are considered to reflect local tissue densities [21].

Deformation-based morphometry

VBM enables one to identify the *location* of a morphological difference between groups, but it can be difficult to interpret the underlying cause of the difference (i.e. could be due to a change in tissue density or volume). DBM complements VBM because it estimates a surrogate of local brain volume relative to the MNI152 template, which allows for the underlying cause of difference to be interpreted [23]. It consists of spatially transforming each MRI non-linearly to the MNI152 template and provides a deformation field [24]. To characterize volumetric growth and shrinkage, the voxel-wise Jacobian determinant of the deformation field was computed [23].

Cortical modeling

Both VBM and DBM are dependent on automated non-linear registration procedures to map each voxel of an individual's MRI to its corresponding location on an atlas brain. This procedure can sometimes fail when applied to the cortex due to wider inter-individual variability in cortical morphology, reducing its effectiveness to detect cortical volume differences. To overcome this limitation, cortical modeling provides a direct quantitative index of cortical thickness useful for detecting subtle cortical thickness differences [25]. Fast Accurate Cortical Extraction (FACE) was used to extract the cortical surface and measure the cortical thickness by deforming polygonal meshes to fit the gray-white matter and pial surface boundaries [26]. Thickness estimates were mapped to the MNI152 average cortical template using non-linear surface registration tools that are more effective than existing registration tools used for VBM and DBM [27]. This was followed by blurring each thickness map with a 20 mm surface-based kernel.

Statistical analyses

Voxel-wise general linear models (GLM) were used to compare whole brain maps for Jacobian determinants, tissue densities, and cortical thickness estimates between the HIV-infected and HIV-uninfected group. Additionally, a series of GLM were used to examine the relationship between brain maps and the following HIV-related factors within the HIV-infected group: nadir CD4, current CD4, current plasma viral load, viral suppression status (detectable versus undetectable), CPE score, treatment status (treated versus untreated), and cognitive function as summarized by Rasch analysis. For each model age, gender, ethnicity, and education were included as covariates to account for variance in brain volumes (overview of model found in supplementary materials). All models controlled for multiple comparisons by using the standard false discovery rate (FDR) with a false-positive rate of 5% [28]. FDR accounts for multiple comparisons by controlling the number of false positives. It is applied to the uncorrected whole brain statistical maps, where surviving voxels are considered to be statistically significant. A false-positive rate of 5% implies that no more than 5% of all surviving voxels are false positives.

Results

Demographics

Table 1 summarizes cohort demographics, neuropsychological performance, and clinical characteristics. The majority (75%) of HIV-infected patients had effective viral suppression (<50 copies/mL), and 90% were currently receiving stable HAART. Although the two groups were demographically similar, HIV-infected patients performed significantly worse than HIV-uninfected subjects on neuropsychological testing, whether summarized by NPZ-4 or Rasch scoring ($p < 0.001$).

Neuropsychological performance

VBM and DBM analysis revealed that poorer neuropsychological performance in the HIV-infected group, as quantified by Rasch analysis, was strongly correlated with larger lateral ventricle volume ($p < 0.04$). Cortical modeling also revealed a strong relationship between

poorer neuropsychological performance and cortical thickness reductions in the left lateral temporal pole, left inferior occipital, right lateral occipital and right inferior lateral frontal cortices in the HIV-infected group ($p < 0.03$) (Figure 1).

HIV-infected versus HIV-uninfected

VBM analysis demonstrated that HIV-infected patients had significant reductions in WM densities in the brainstem and thalamus compared to the HIV-uninfected group ($p < 0.03$) (Figure 2). No significant tissue density differences in the GM or CSF maps were detected. DBM analysis did not reveal significant volumetric differences between the HIV-infected and HIV-uninfected groups. However, regional patterns of brain volume loss were similar to those seen with VBM when a more lenient statistical threshold was utilized ($p < 0.1$) (supplementary material Figure S2). Cortical modeling revealed significant cortical thickness reductions in the HIV-infected group compared to the HIV-uninfected group ($p < 0.02$) (Figure 3). The most pronounced reductions were seen bilaterally in the temporal and frontal lobes, and right primary motor and sensory cortex. On the medial surfaces, significant cortical thickness reductions were seen in the posterior cingulate, orbitofrontal cortex, and left anterior cingulate.

Nadir CD4

VBM and DBM analysis revealed significant reductions in WM densities and volumes, respectively, in the brainstem, globus pallidus, internal capsule, caudate, and right frontal lobe associated with lower nadir CD4 ($p < 0.01$). Lower nadir CD4 was also significantly associated with greater CSF volume in the third ventricle (Figure 4A/B). In contrast, nadir CD4 was not significantly associated with changes in cortical thickness.

Current CD4

There were no detectable volumetric or cortical thickness changes associated with current CD4. Additional analysis controlling for historical effects of HIV infection (i.e. nadir CD4) was performed. Similarly, no significant effects were observed.

Current Plasma Viral Load

Current viral loads and viral suppression status (detectable versus undetectable viral loads) were not significantly correlated with any brain volume or cortical thickness estimates.

Treatment Effects

No significant differences were observed for regional brain volume and cortical thickness estimates in treated and untreated HIV-infected participants. Moreover, no significant correlations were observed between CPE scores and brain volumetric measures.

Discussion

In this study, we took advantage of multiple neuroimaging methods to investigate the spatial distribution of cortical and subcortical volume loss in a group of HIV-infected individuals in the HAART era. We observed significant reductions in cortical thickness throughout the cortex and WM tissue densities in subcortical structures, and worse cognitive performance in

the HIV-infected cohort. HIV-infected patients with a history of more severe immunosuppression had significantly smaller subcortical volumes, but this variable was not related to cortical thickness reductions. In contrast, worse cognitive performance was associated with reduced regional cortical thickness but not subcortical volumes. The results presented provide a detailed characterization of the pattern and extent of brain injury in a diverse group of HIV-infected patients.

Patterns of reduced subcortical integrity were observed in HIV-infected patients compared to a demographically similar HIV-uninfected group. Most notably, VBM analysis revealed reductions in WM tissue density in the brainstem and thalamus. These results are consistent with several prior studies that have reported volume loss in similar regions [7,11,13,29,30], including diffusion tensor imaging studies that show loss of WM integrity in the thalamus and brainstem of HIV-infected patients [31,32]. The findings here support the hypothesis that subcortical structures are particularly vulnerable to the virus [33], and add spatial detail regarding the distribution of atrophy. Although DBM did not reveal any significant group differences, regional patterns of volumetric loss similar to those seen with VBM were evident at more lenient statistical thresholds. This argues that the observed subcortical differences primarily reflect reductions in WM tissue density rather than volumetric shrinkage, which implies that the underlying pathophysiology may particularly target WM. This also demonstrates the advantage of using VBM and DBM together [23].

While VBM and DBM have the potential to detect cortical volume changes, variability in cortical folding patterns may lead to suboptimal spatial normalization, reducing the statistical power to detect subtle cortical changes. Cortical modeling overcomes this limitation by smoothing highly variable cortical folds and utilizing cortical depth maps to optimally align homologous cortical regions. Cortical modeling revealed that HIV-infected patients had thinner cortices in the temporal and frontal lobes on both hemispheres, right primary motor and sensory cortex, posterior cingulate, orbitofrontal cortex, and left anterior cingulate cortex. The observed cortical thickness differences support findings from a limited number of cortical modeling studies suggesting that HIV infection can lead to significant cortical-based changes [34-36].

The HIV-infected group performed significantly worse than demographically similar HIV-uninfected individuals on neuropsychological tests, adding to the growing body of evidence that suggests HIV-related cognitive impairment remains frequent despite effective treatment and minimal comorbidities [1]. Regional cortical thickness reductions were related to poorer neuropsychological performance in the left lateral temporal pole, left inferior occipital, right lateral occipital and right inferior lateral frontal cortices, effects that presumably reflect the regions engaged by the particular set of cognitive tests administered. In contrast, subcortical volume changes were not significantly related to overall performance. These differential results may reflect the fact that the neuropsychological tests that were administered primarily assess cortical-hemispheric functions and might be less sensitive to subcortical dysfunction, *a priori*.

To assess whether brain volume changes were influenced by variables related to the infection, brain volumes were correlated with nadir CD4, current CD4, viral load, and CPE

measures within the HIV-infected group. VBM and DBM analysis revealed that HIV-infected patients with a history of more severe immunosuppression, indexed by nadir CD4, had significant reductions in WM density and smaller volumes in the brainstem, thalamus, caudate, putamen, globus pallidus, internal capsule and right frontal lobe, as well as greater enlargement of the third ventricle. This finding is consistent with the existing literature [9,11,37-40] supporting the theory that volume loss, in part, occurs during the time of untreated infection [8,12] suggesting that early initiation of HAART might be beneficial for long term brain integrity. Longitudinal data is required to determine whether these are static changes, arrested by HAART, or continue to develop despite HAART.

Interestingly cortical modeling did not reveal any cortical thickness reductions associated with the severity of immunosuppression. This confirms, in a much larger sample, the results of a prior cortical modeling study, which likewise found no relationship between the cortical thickness estimates and nadir CD4 [35]. The differential results argues that the underlying pathogenesis of injury between subcortical and cortical structures may be different or progress at different rates in the presence of the virus [35,41]. In particular, cortical thinning may be secondary to subcortical dysfunction [36] possibly mediated by subcortical WM destruction [35]. However, the underlying pathophysiology of cortical thinning in HIV-infected patients remains unknown, and should be addressed in future work.

The association between brain volumes and nadir CD4 reported here add further weight to a considerable body of existing evidence. However, there is less consensus as to the relationship between other HIV-related factors (current CD4, viral load, and treatment status) and brain structural measures. Inconsistencies likely reflect differences in degree of infection severity in HIV cohorts, as well as limitations of sample size and imaging analytic approaches, with most studies relying on a single method. Here, the large sample with wide variance in HIV-related variables, and the comprehensive approach to characterizing regional brain volumes are strengths that allow the brain volume relations with current CD4, viral load, and treatment status to be thoroughly explored.

Despite the power afforded by the large sample size, indices of current infection severity, including current CD4, viral load, and viral suppression status, were not associated with subcortical or cortical changes. While a few studies have reported that increasing viral loads were associated with decreased caudate, thalamus, frontal and parietal lobe volumes [9,37], accumulating reports in the HAART era have not detected such relationships [7,8,12,34,35,39] suggesting that the use of blood markers, particularly plasma viral loads, may not be sensitive enough to monitor brain injury once treatment is initiated. However, the current study may not have detected such relationships due to the small number of HIV-infected patients with detectable viral loads (n=31), with few patients (n=9) having high viral loads (>1000 copies/mL). Further studies are needed to clarify whether plasma viral load relates reliably to brain integrity in patients with poor control despite HAART.

The effects of HAART on brain integrity were assessed by comparing brain volume estimates in treated and untreated HIV-infected patients, and correlating with CPE scores. No significant differences, or correlations, with any volumetric measures were revealed. Although this finding is consistent with prior studies, and suggests that higher penetrating

regimens do not significantly influence brain volumes [7,12,29,39], this study was not designed to determine the neuro-protective or toxic effects of HAART. The small untreated group (n=13) and limited number of regimens prescribed to most participants (average CPE Score = 6.70 ± 2.85) means that this sample is not well suited to address this question. Studies with larger variability of treatment regimens would be needed to fully test this hypothesis.

This study has limitations. First, causal inferences cannot be made based on cross-sectional data. Validation of these results and unraveling the underlying pathogenesis of brain dysfunction will require longitudinal studies that track brain volumes from primary to chronic HIV infection. Second, recent evidence has found that cardiovascular risk factors are elevated in HIV-infected patients, particularly those with longer infection and treatment duration, and were related to WM damage and cognitive deficits [42]. Unfortunately, data on cardiovascular risk factors were not acquired in the present study, so the possibility of vascular injury causing the observed changes cannot be fully discounted. Further work is needed to establish the contribution of vascular injury to brain structure and function.

In conclusion, this study applied multiple advanced analytic approaches to explore the spatial distribution of changes on brain structure in HIV-infected patients in the HAART era. Significant volume reductions were detected in the HIV-infected group, primarily in subcortical WM, and these reductions were associated with previous episodes of immunosuppression. Regionally specific reductions in cortical thickness were also detected between HIV-infected and uninfected groups. However, the cortical thickness reductions were not predicted by nadir CD4. Collectively, the results reported here suggests that distinct mechanisms may underlie subcortical and cortical injury, and demonstrates that subcortical injury most likely occurs during the time of untreated infection suggesting that treatment with HAART as early as possible might mitigate brain injury. Longitudinal investigations to confirm these reports are warranted.

Supplementary Material

Refer to Web version on PubMed Central for supplementary material.

Acknowledgments

References

1. Heaton RK, Clifford DB, Franklin DR, et al. HIV-associated neurocognitive disorders persist in the era of potent antiretroviral therapy: CHARTER Study. Neurology. 2010; 75(23):2087–2096. [PubMed: 21135382]

2. Mothobi NZ, Brew BJ. Neurocognitive dysfunction in highly active antiretroviral therapy era. Curr Opin Infect Dis. 2012; 25(1):4–9. [PubMed: 22156897]

3. Holt JL, Kraft-Terry SD, Chang L. Neuroimaging studies of the aging HIV-1-infected brain. J Neurovirol. 2012; 18(4):291–302. [PubMed: 22653528]

4. Ances BM, Hammoud DA. Neuroimaging of HIV Associated Neurocognitive Disorders (HAND). Curr Opin HIV AIDS. 2014; 9(6):545–551. [PubMed: 25250553]

5. Thompson PM, Jahanshad N. Novel Neuroimaging Methods to Understand How HIV Affects the Brain. Curr HIV/AIDS Rep. 2015; 12(2):289–298. [PubMed: 25902966]

6. Castelo JMB, Courtney MG, Melrose RJ, et al. Putamen Hypertrophy in Nondemented Patients With Human Immunodeficiency Virus Infection and Cognitive Compromise. Arch Neurol. 2007; 64(9):1275–1280. [PubMed: 17846265]

7. Chiang M, Dutton RA, Hayashi KM, et al. 3D pattern of brain atrophy in HIV/AIDS visualized using tensor-based morphometry. Neuroimage. 2007; 34(1):44–60. [PubMed: 17035049]

8. Becker JT, Sanders J, Madsen SK, et al. Subcortical brain atrophy persists even in HAART-regulated HIV disease. Brain Imaging Behav. 2011; 5(2):77–85. [PubMed: 21264551]

9. Cohen RA, Harezlak J, Schifitto G, et al. Effects of NadirCD4 Count and Duration of HIV Infection on Brain Volumes in the HAART Era. J Neurovirol. 2010; 16(1):25–32. [PubMed: 20113183]

10. Becker JT, Maruca V, Kingsley LA, et al. Factors affecting brain structure in men with HIV disease in the post-HAART era. Neuroradiology. 2012; 54(2):113–121. [PubMed: 21424708]

11. Kallianpur KJ, Shikuma C, Kirk GR, et al. Peripheral blood HIV DNA is associated with atrophy of cerebellar and subcortical gray matter. Neurology. 2013; 80(19):1792–1799. [PubMed: 23596064]

12. Ances BM, Orteg M, Vaida F, et al. Independent Effects of HIV, Aging and HAART on Brain Volumetric Measures. J Acquir Immune Defic Syndr. 2012; 59(5):469–477. [PubMed: 22269799]

13. Janssen MAM, Meulenbroek O, Steens SCA, et al. Cognitive function, wellbeing and brain correlates in HIV-1 infected patients on long-term combination antiretroviral therapy. AIDS. 2015; 29:2139–2148. [PubMed: 26544578]

14. Letendre S, Marquie-Beck J, Capparelli E, et al. Validation of CNS Penetration-Effectiveness Rank for Quantifying Antiretroviral Penetration into the Central Nervous System. Arch Neurol. 2008; 65(1):65–70. [PubMed: 18195140]

15. Heaton RK, Franklin DR, Ellis RJ, et al. HIV-associated neurocognitive disorders before and during the era of combination antiretroviral therapy: Differences in rates, nature and predictors. J Neurovirol. 2011; 17(1):3–16. [PubMed: 21174240]

16. Brouillette M, Mayo N, Fellows LK, et al. A better screening tool for HIV-associative neurocognitive disorders: is it what clinicians need? AIDS. 2015; 29:895–902. [PubMed: 25291105]

17. Coupe P, Yger P, Prima S, et al. An optimized blockwise nonlocal means denoising filter for 3D magnetic resonance images. IEEE Trans Med Imaging. 2008; 27(4):425–441. [PubMed: 18390341]

18. Sled JG, Zijdenbos AP, Evans AC. A nonparametric method for automatic correction of intensity nonuniformity in MRI data. IEEE Trans Med Imaging. 1998; 17(1):87–97. [PubMed: 9617910]

19. Eskildsen SF, Coupe P, Fonov V, et al. BEaST: Brain Extraction based on nonlocal Segmentation Technique. Neuroimage. 2012; 59(3):2362–2373. [PubMed: 21945694]

20. Collins DL, Neelin P, Peters TM, et al. Automatic 3D intersubject registration of MR volumetric data in standardized Talairach space. J Comput Assist Tomogr. 1994; 18(2):192–205. [PubMed: 8126267]

21. Ashburner J, Friston KJ. Voxel-Based Morphometry - The Methods. Neuroimage. 2000; 11(6): 805–821. [PubMed: 10860804]

22. Zijdenbos AP, Forghani R, Evans AC. Automatic 'pipeline' analysis of 3-D MRI data for clinical trials: application to multiple sclerosis. IEEE Trans Med Imaging. 2002; 21(10):1280–1291. [PubMed: 12585710]

23. Ashburner J, Hutton C, Frackowiak R, et al. Identifying Global Anatomical Differences: Deformation-Based Morphometry. Hum Brain Mapp. 1998; 6(5-6):348–357. [PubMed: 9788071]

24. Collins DL, Holmes CJ, Peters TM, et al. Automatic 3-D Model-Based Neuroanatomical Segmentation. Hum Brain Mapp. 1995; 3(3):190–208.

25. Lyttelton O, Boucher M, Robbins S, et al. An unbiased iterative group registration template for cortical surface analysis. Neuroimage. 2007; 34(4):1535–1544. [PubMed: 17188895]

26. Eskildsen SF, Østergaard LR. Active Surface Approach for Extraction of the Human Cerebral Cortex from MRI. Paper presented at: Medical Image Computing and Computer-Assisted Intervention. 2006

27. Collins, DL., Le Goualher, G., Evans, AC. Non-linear cerebral registration with sulcal constraints. In: Wells, WM.Colchester, A., Delp, S., editors. Medical Image Computing and Computer-Assisted Intervention — MICCAI'98: First International Conference Cambridge, MA, USA, October 11–13, 1998 Proceedings. Berlin, Heidelberg: Springer Berlin Heidelberg; 1998. p. 974-984.

28. Genovese CR, Lazar NA, Nichols T. Thresholding of Statistical Maps in Functional Neuroimaging Using the False Discovery Rate. Neuroimage. 2002; 15(4):870–878. [PubMed: 11906227]

29. Küper M, Rabe K, Esser S, et al. Structural gray and white matter changes in patients with HIV. J Neurol. 2011; 258(6):1066–1075. [PubMed: 21207051]

30. Wade BSC, Valcour VG, Wendelken-Riegelhaupt L, et al. Mapping abnormal subcortical brain morphometry in an ederly HIV+ cohort. Neuroimage Clin. 2015; 9:564–573. [PubMed: 26640768]

31. Nir TM, Jahanshad N, Busovaca E, et al. Mapping white matter integrity in elderly people with HIV. Hum Brain Mapp. 2014; 35(3):975–992. [PubMed: 23362139]

32. Wright PW, Vaida FF, Fernández RJ, et al. Cerebral white matter integrity during primary HIV infection. AIDS. 2015; 29(4):433–442. [PubMed: 25513818]

33. Ances BM, Ellis RJ. Dementia and Neurocognitive Disorders Due to HIV-1 Infection. Semin Neurol. 2007; 27(1):86–92. [PubMed: 17226745]

34. Thompson PM, Dutton RA, Hayashi KM, et al. Thinning of the cerebral cortex visualized in HIV/AIDS reflects CD4+ T lymphocyte decline. Proc Natl Acad Sci USA. 2005; 102(43):15647–15652. [PubMed: 16227428]

35. Kallianpur KJ, Kirk GR, Sailasuta N, et al. Regional Cortical Thinning Associated with Detectable Levels of HIV DNA. Cereb Cortex. 2011; 22(9):2065–2075. [PubMed: 22016479]

36. duPlessis S, Vink M, Joska JA, et al. Prefrontal cortical thinning in HIV infection is associated with impaired striatal functioning. J Neural Transm. 2016:1–9. [PubMed: 26724924]

37. Cardenas VA, Meyerhoff DJ, Studholme C, et al. Evidence for ongoing brain injury in human immunodeficiency virus-positive patients treated with antiretroviral therapy. J Neurovirol. 2009; 15(4):324–333. [PubMed: 19499454]

38. Jernigan TL, Archibald SL, Fennema-Notestine C, et al. Clinical factors related to brain structure in HIV: the CHARTER study. J Neurovirol. 2011; 17(3):248–257. [PubMed: 21544705]

39. Hua X, Boyle CP, Harezlak J, et al. Disrupted cerebral metabolite levels and lower nadir CD4+ counts are linked to brain volume deficits in 210 HIV-infected patients on stable treatment. Neuroimage Clin. 2013; 3:132–142. [PubMed: 24179857]

40. Pfefferbaum A, Rosenbloom MJ, Sassoon SA, et al. Regional Brain Structural Dysmorphology in HIV Infection: Effects of AIDS, Alcoholism, and Age. Biol Psychiatry. 2012; 72(5):361–370. [PubMed: 22458948]

41. Moore DJ, Masliah E, Rippeth JD, et al. Cortical and subcortical neurodegeneration is associated with HIV neurocognitive impairment. AIDS. 2006; 20(6):879–887. [PubMed: 16549972]

42. Kuller LH, Lopez OL, Newman A, et al. Risk factors for dementia in the cardiovascular health cognition study. Neuroepidemiology. 2003; 22(1):13–22. [PubMed: 12566949]
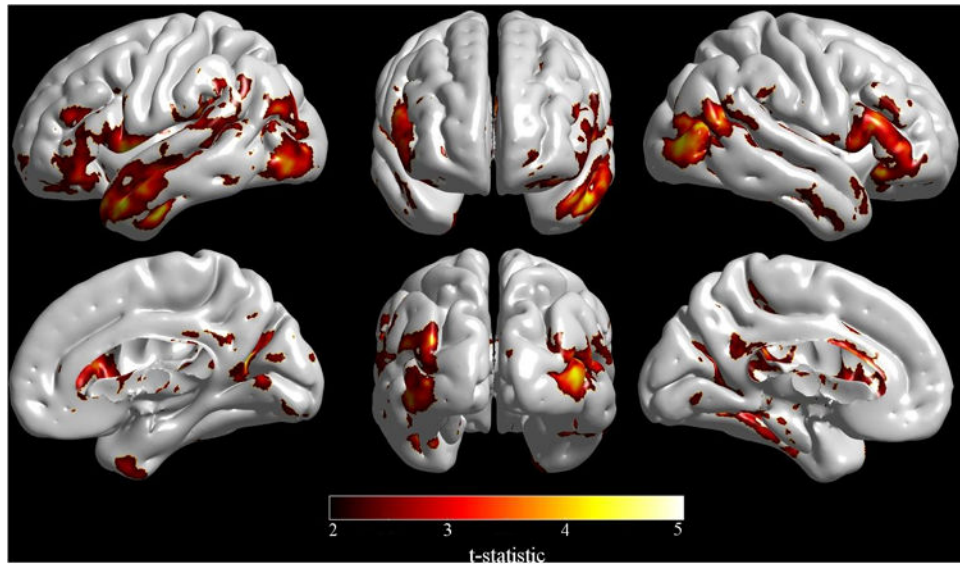
Figure 1.
Reductions in cortical thickness in HIV-infected patients were associated with worse neuropsychological performance (as indexed by Rasch scoring) in the left lateral temporal pole, left inferior occipital, right lateral occipital, and right inferior lateral frontal cortices. (Image created with SurfStat http://www.math.mcgill.ca/keith/surfstat/).
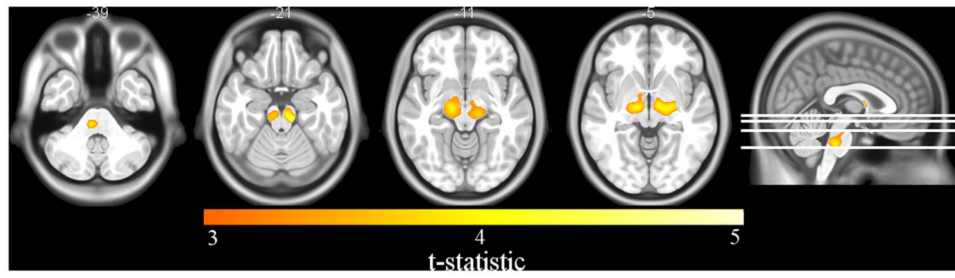
Figure 2.
Axial slices of voxel-based morphometry (VBM) differences in HIV-infected compared to HIV-uninfected subjects. Reductions in WM were detected in the brainstem and thalamus. (Image created with MRIcron http://people.cas.sc.edu/rorden/mricron/index.html)
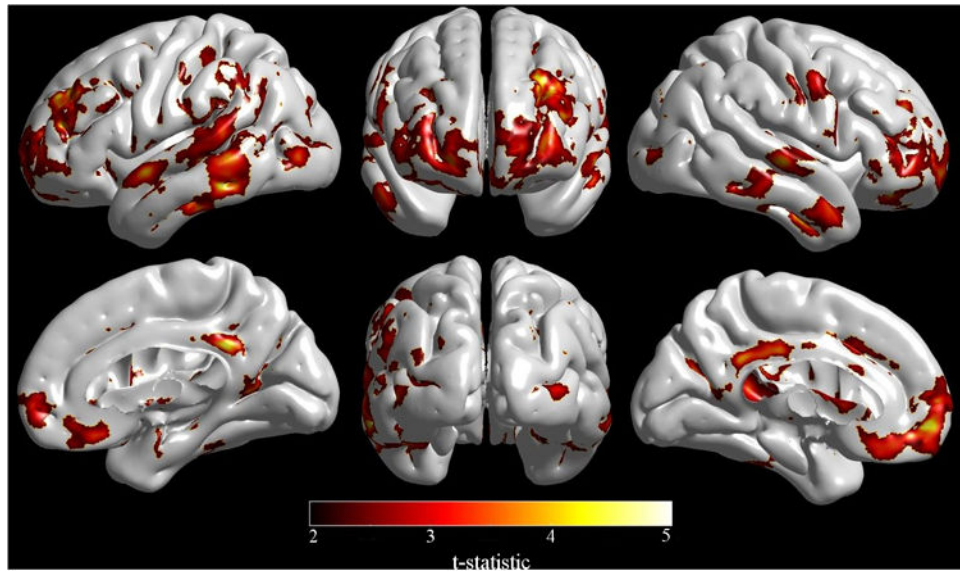
Figure 3.
Cortical modeling showed significant cortical thickness reductions in HIV-infected patients compared to HIV-uninfected participants specifically within the right primary motor and sensory cortex, lateral temporal and frontal lobes, and posterior cingulate, orbitofrontal cortex and left anterior cingulate. (Image created with SurfStat http://www.math.mcgill.ca/keith/surfstat/).
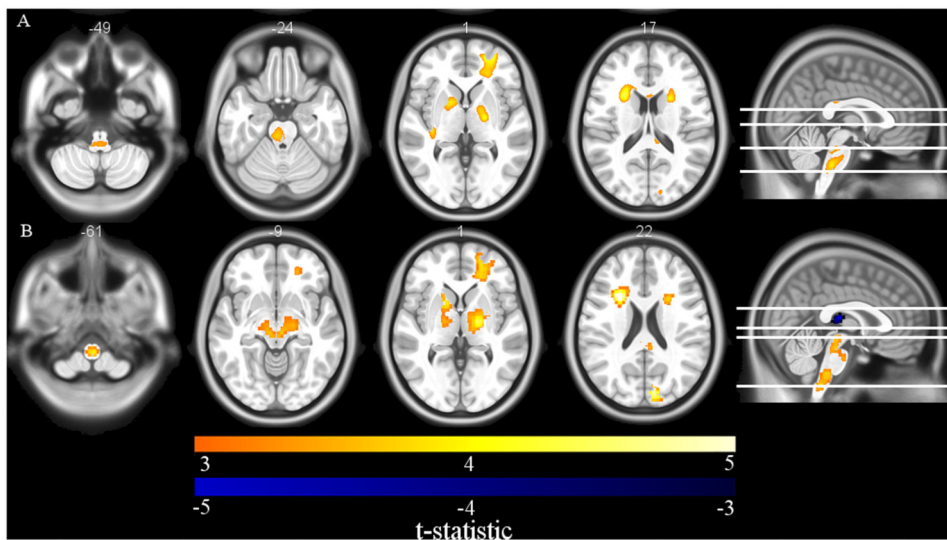
Figure 4.
A) Axial slices of voxel-based morphometry (VBM) results show significant WM reductions in the brainstem, globus pallidus, internal capsule, caudate, and right frontal lobe that were associated with lower nadir CD4 in HIV-infected patients. B) Deformation-based morphometry (DBM) revealed an association between lower nadir CD4 and smaller volumes in the brainstem, thalamus, caudate, putamen, globus pallidus and right frontal lobe, and enlargement of the third ventricle in HIV-infected patients. (Images created with MRIcron http://people.cas.sc.edu/rorden/mricron/index.html).

Table 1

Demographic, medical, neuropsychological, and laboratory values for all subjects

	HIV-infected (n=125)	HIV-uninfected (n=62)	P value [a]
Demographics			
Age [(years), mean (SD)]	47.2 ± 12.2	45.4 ± 11.9	0.10
Sex [n (% male)]	80 (64)	34 (55)	0.27
Education [(years), mean (SD)]	14.4 ± 2.6	14.5 ± 2.2	0.25
Ethnicity [n (%)]			0.31
African American	84 (67)	38 (62)	
Caucasian	41 (33)	24 (38)	
Past Substance Use [b]			
Marijuana [n (%)]	14 (11)	3 (5)	0.1
Cocaine [n (%)]	4 (3)	0 (0)	0.1
Meth [n (%)]	2 (2)	1 (2)	0.9
Opiates [n (%)]	2 (2)	2 (3)	0.3
Alcohol [n (%)]	10 (8)	3 (5)	0.4
Clinical and Neuropsychological Characteristics			
Estimated duration of HIV infection (years)	10.5 ± 7.8	NA	NA
% receiving highly active antiretroviral therapy (HAART)	90	NA	NA
Central Nervous System Penetration Effectiveness (CPE) Score [mean (SD)]	6.70 ± 2.85	NA	NA
Past hepatitis-C co-infection [n (%)]	3 (2)	NA	NA
Neuropsychological Performance (Rasch Score) [c]	0.14 ± 1.19	1.16 ± 1.08	**< 0.001**
Neuropsychological Performance (NPZ-4) [c]	-0.85 ± 1.27	-0.14 ± 0.91	**< 0.001**
Laboratory			
Current CD4 [(cells/μL), median (IQR)]	533 (267, 724)	NA	NA
Nadir CD4 [(cells/μL), median (IQR)]	189 (40, 308)	NA	NA
Median Log Plasma Viral Load [(copies/mL), median (IQR)]	1.31 (1.30, 1.94)	NA	NA
% Virologically Suppressed (<50 copies/mL)	75	NA	NA

[a] Group comparisons using Student's t test (age, education, and neuropsychological performance (Rasch score and NPZ-4), and Fisher's exact test (gender, ethnicity, and past substance use).

[b] History of past substance use based on participant self-report.

[c] Higher scores indicate better performance on neuropsychological test